On the stability of hole states in molecules and clusters

Reinhard, P. G., Dinh, P. M., Dundas, D., Suraud, E., & Vincendon, M. (2022). On the stability of hole states in molecules and clusters. *European Physical Journal: Special Topics*, *232*, 2095-2099. Advance online publication. https://doi.org/10.1140/epjs/s11734-022-00676-6

Published in:
European Physical Journal: Special Topics

Document Version:
Peer reviewed version

Queen's University Belfast - Research Portal:
Link to publication record in Queen's University Belfast Research Portal

EPJ manuscript No.
(will be inserted by the editor)

On the stability of hole states in molecules and clusters

P.-G. Reinhard[1], P. M. Dinh[2], D. Dundas[3], E. Suraud[2], M. Vincendon[2]

[1] Institut für Theoretische Physik, Universität Erlangen, D-91058 Erlangen, Germany
[2] Laboratoire de Physique Théorique, Université de Toulouse, CNRS, UPS, F-31062 Toulouse Cedex, France
[3] School of Mathematics and Physics, Queen's University Belfast, University Road, Belfast BT7 1NN, N. Ireland

the date of receipt and acceptance should be inserted later

Abstract Recent investigations of the electron dynamics of molecules after irradiation with a short, strong XUV pulse have shown that under certain conditions, a rather clean deep hole state can be generated which, in turn, leads to a remarkable dipole instability. Here we analyze in more depth the dipole instability, simplifying the excitation mechanism by instantaneous generation of a hole in one of the occupied states of the system. We investigate how the dipole instability depends on the system, the state in which the hole is cut, and the amount of depletion which is given to the hole state. We also quickly discuss the mechanism beyond the dipole instability in analogy to the generation of a coherent photon field in a laser.

PACS. XX.XX.XX No PACS code given

The steady progress in the development of light sources provides us with ever shorter photon pulses down into the attosecond regime. This opens a world of new possibilities in analyzing electronic dynamics at short time scales, see, e.g., [1,2,3,4]. A detailed theoretical description of the ultrashort excitation processes is cumbersome and one often simplifies the initial phase by assuming that an attosecond XUV pulse instantaneously removes an electron from one of the occupied states, see, e.g., [5,6,7,8,9,10]. Very recently, we have simulated the excitation process by extremely short XUV pulses in detail and were able to find dynamical regimes in which the short pulse indeed manages to produce almost instantaneously a hole in a deep lying electron state, thus delivering justification of the simplified excitation model by instantaneous hole creation [11]. As an unexpected side-effect of this study, we observed a remarkable dipole instability, i.e. a spontaneous generation of strong dipole oscillation fed by the deep lying hole state. The aim of this contribution is to study this dipole instability in more detail, discussing the underlying mechanism and considering dependence on system, hole state, and initial excitation energy. To focus on the dynamics after hole generation, we simplify the excitation process (as in many earlier works [12,6]) to an instantaneous hole initialization.

Before presenting results, we briefly summarize the formal and numerical background. We use time-dependent density functional theory at the level of the time-dependent local density approximation (TDLDA) [13] with the energy density functional of Ref. [14] augmented by an averaged self interaction correction to obtain approximately correct single particle energies [15,16,17,18]. Only valence electrons are described explicitly. The coupling to the ionic cores is mediated by a pseudopotential of Goedeker type [19]. The ionic positions are kept frozen in view of the short time scales considered here. The calculations are performed with the code published and explained in great detail in [20]. The single electron wave functions $\varphi_\alpha(\mathbf{r})$ and other spatial fields are represented on a 3D Cartesian grid with a grid spacing sufficiently fine to resolve the pseudopotentials: 0.3 a_0 for covalent molecules and 0.8 a_0 for metal clusters. The stationary electronic state is computed using an accelerated gradient method and the time-dependent Kohn-Sham equations are propagated using a time-splitting technique with time step corresponding to grid spacing, e.g., between 0.0048 and 0.0096 fs. The dynamical evolution is initialized by removing instantaneously an electron (or a fraction thereof) from the lowest occupied state and the thus excited system is propagated without applying any further external field.

First, a quick glance at system dependence of the dipole instability. We have investigated dynamics after generating instantaneously a hole in the deepest valence state (denoted here $\alpha = 1$) for a great variety of atoms and molecules with all sorts of binding. So far, the dipole instability was seen in many systems but not in others. A typical selection is shown in Fig. 1 which depicts the time evolution of the dipole signal, for better visibility a logarithmic scale is used. Two systems (Na_9^+ and H_2O) are polar molecules having finite dipole moment in the ground state while N_2 has not. N_2 and H_2O represent covalent binding and Na_9^+ metallic binding. The middle panel shows the results for N_2 which has the simplest structure of the three molecules here. The dipole instability is clearly seen for the direction along the molecular axis and nothing occurs orthogonal to it. That is plausi-

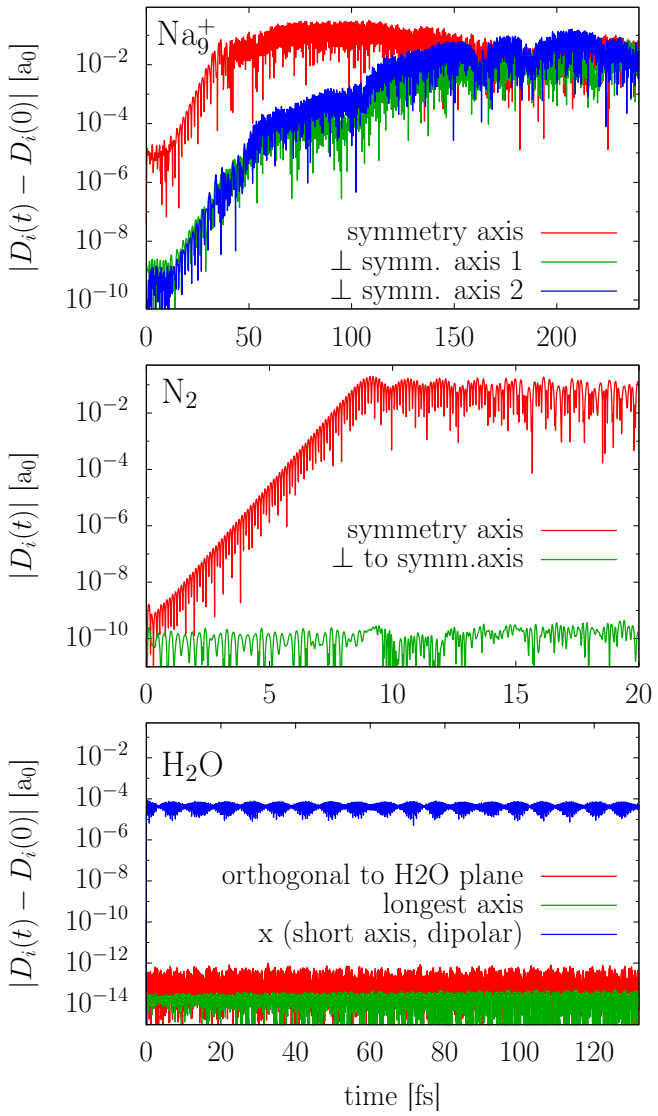

Figure 1. Dipole signal in all three spatial directions after instantaneous initialization of a hole in the lowest occupied state ($\alpha = 1$) for three different systems and the different spatial directions in each system. For the polar molecules H_2O and Na_9^+, the initial finite dipole moment $D_i(0)$ is subtracted.

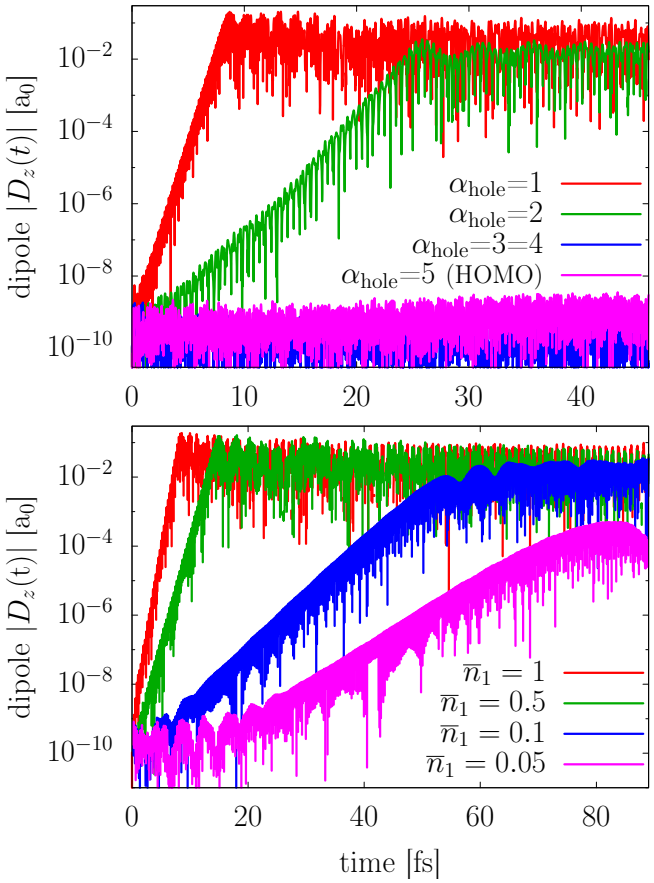

Figure 2. Time evolution of dipole moment along the symmetry axis for N_2 for various initial conditions. Upper panel: variation of hole state as indicated. Lower panel: variation of initial depletion, denoted by $\overline{n}_1$,for a hole in the $\alpha = 1$ state.

ble because N_2 is more extended along its axis and so has large dipole matrix elements in that direction. The time scale of growth is considerably short, one order of magnitude variation in about 1.2 fs. This is faster than the scale of dynamical electron correlations which means that the instability persists also for treatment beyond TDLDA as we had shown in [11].

The other covalent molecule in Fig. 1 is H_2O. This does not show any trace of dipole instability. Mind that we have computed it for long time to exclude a later appearance. Much longer does not make sense because the time scale for electronic dissipation from dynamical correlations is about 5 fs for that system and excitation energy. That would erase any spontaneous dipole which grows so slowly. One may speculate that the finite dipole moment of H_2O acts as a hindrance for the dipole instability. But this cannot be the case as our other polar molecule, Na_9^+ (upper panel in Fig. 1) shows the dipole instability in all three directions. Here we note that the signal in the polar direction (along the static dipole) starts with larger initial fluctuations than in the other two directions because both systems (Na_9^+ and H_2O) are much softer in the polar mode. To mention other systems, we have seen the dipole instability in C_2H_2 and the Ar atom, but not in C_2H_4 and C_{60}. It remains a task for future studies to develop a simple estimate of growth rate and, with it, of the appearance of an instability. In all cases discussed here, the growth of dipole oscillations levels off if the energy from the initial excitation is used up.

The first aspect we investigate is the dependence of the instability on the initial state. This covers two aspects. The first one is the target state itself, namely we explore whether the instability is linked to the original target hole state. Another complementary aspect is the amount of depletion of this state, namely whether the hole excitation is complete or not. The upper panel of Fig. 2 addresses the dependence of the dipole instability on the initial hole state. N_2 has 2×5 occupied (spin-degenerate)

electron states with energies $\varepsilon_1 = -33.5$ eV, $\varepsilon_2 = -18.6$ eV, $\varepsilon_3 = \varepsilon_4 = -16.9$ eV, $\varepsilon_5 = -15.1$ eV. The states 1,2, and 5 have azimuthal, orbital angular momentum component $m = 0$, while the degenerate pair 3 and 4 have $m = \pm 1$. The initial excitation energy is approximately $\varepsilon_5 - \varepsilon_\alpha$ plus a small polarization correction from the mean-field interaction. Holes in $\alpha = 3, 4$, or 5 do not produce the instability, probably because their excitation energy is too small, while the two lowest states do carry sufficient excitation energy. However, there is a marked difference between these two states: the hole in $\alpha = 1$ has much faster growth and leads to larger final amplitude. Both behaviors are plausible because a hole in $\alpha = 1$ carries six time larger excitation energy than a hole in $\alpha = 2$. Not only does the growth rate differ between the hole in $\alpha = 1$ and $\alpha = 2$, but also the oscillation frequency, as one can deduce from the figure. Spectral analysis of the dipole oscillations (not shown here) shows that their frequency lies close to the energy difference between the hole state and the HOMO. This was found also for other system as, e.g., those from Fig. 1.

The lower panel of Fig. 2 deals with the amount of depletion given to the initial $\alpha = 1$ hole, denoted by $\overline{n}_1$. In that case, we did not always remove one full electron from the $\alpha = 1$ state but only a fraction thereof by reducing its occupation weight gradually. The amount of reduction is called the depletion $\overline{n}_1$. Note that the initial excitation energy is proportional to $\overline{n}_1$. This immediately explains what we see in the figure. Both the growth rate and final amplitude decrease with decreasing depletion $\overline{n}_1$. It is surprising that the dipole instability appears even for the lowest depletion $\overline{n}_1 = 0.05$ whose excitation energy is about 20 times smaller than that for $\overline{n}_1 = 1$. Note that the rate of growth and the final dipole amplitude sensitively depend on excitation energy. But they depend also on the degree of coupling between the excited two-level subsystem and the other modes as we can learn from comparing H_2O with N_2 which have the same excitation energy but different outcome (one with the other without dipole instability).

Within the limited space of this contribution, we very briefly sketch the mechanism beyond the dipole instability. The dipole signal develops as an exponentially growing envelope with regular dipole oscillations underneath. That is more involved than the simple exponential growth as one would expect from a classical instability. It is a quantum mechanical instability starting from occupation inversion in a two-level system, here the transition between the deepest single particle state and a higher lying state near the Fermi energy which has large dipole transition moment with the deepest state. For the present example N_2, these are the states $\alpha = 1$ and $\alpha = 2$ (same angular momentum $m = 0$ and different parity). Mapped to the two-level model (see the levels mentioned above), a hole in state $\alpha = 1$ is the excited state $\varphi_\uparrow$ of the model and a hole in $\alpha = 2$ corresponds to its ground state $\varphi_\downarrow$ (we employ here spin notation $\uparrow\downarrow$ to indicate that a two-level model is isomorphous to a spin system). If the two-level system were isolated, it would remain in the excited configuration $\varphi_\uparrow$ having zero dipole moment. In practice, it couples to other modes of the system such that energy flows away from the two-level system creating a mixed state $\sqrt{1-c_\downarrow^2}\ \varphi_\uparrow + c_\downarrow e^{\mathrm{i}\varepsilon_{\uparrow\downarrow}t}\varphi_0$ (where $\varepsilon_{\uparrow\downarrow}$ is the energy difference between the two states) which has a finite dipole moment. Slowly increasing $c_\downarrow$ stands for the increasing dipole amplitude while the phase factor $e^{\mathrm{i}\varepsilon_{\uparrow\downarrow}t}$ is responsible for the oscillations. In some respects, the mechanism is analogous to symmetry breaking and generation of a coherent dipole field in the laser process [21]. A detailed discussion of this mechanism will be addressed in a future work.

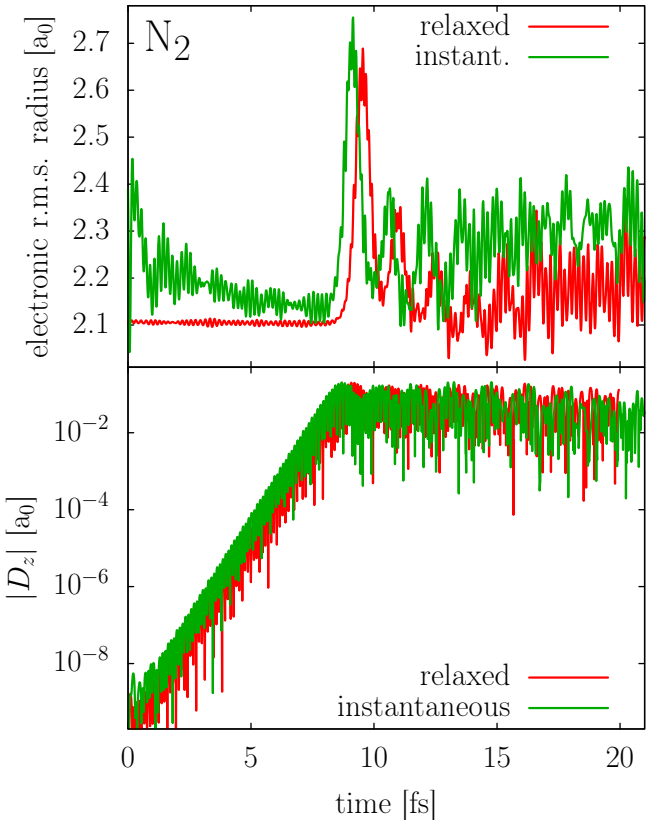

Figure 3. Time evolution of the electronic dipole in direction of the symmetry axis (lower panel) and of the electronic radius $\sqrt{\int \mathrm{d}^3\mathbf{r}\, r^2 \rho_{\mathrm{el}}(\mathbf{r})}$ (upper panel) after instantaneous initialization of a hole in the $\alpha = 1$ state of the N_2 dimer. Compared are the results from initialization by an instantaneous hole (as in all previous examples) and alternatively by cooling the hole configuration to a stationary state.

The instantaneous generation of a hole state leaves the system in unrest and one may wonder to what extent this contributes to the dipole instability. To check this, we produce a cooled hole state by performing static iterations with the constraint that the deepest valence state is kept unoccupied. That cooled state converges and gains order of about 0.1 eV energy as compared to the instantaneous hole state. Figure 3 compares the time evolution of the dipole moment and radius between instantaneous and cooled hole initialization. The dipole moments (lower

panel) stay very close to each other. The cooled initialization manages to have a smaller initial dipole moment, i.e. a smaller seed. Thus both curves have a slight offset but the same slope and final dipole amplitude. The dipole instability is obviously an intrinsic property of the system and not affected by other perturbations.

The time evolution of the radii (upper panel) differs significantly. The instantaneous initialization charges the system at once by one unit producing a Coulomb pressure which, in turn, triggers large radius oscillations. The cooled initialization has managed to re-establish Coulomb equilibrium such that the radius is stable for a long time. The comparison confirms that the dipole instability is independent from many other perturbations in the system. Later on, we see strong radius oscillations appearing around the same time for both initializations. This happens because, at that time, the large dipole oscillations lead to strong electron emission of about 0.6 charge unit. This creates another wave of Coulomb pressure with subsequent radius oscillations.

Finally a word on competing processes. Dynamical electron-electron correlations are known to introduce a dissipation which attenuates the dipole signal [22,23]. Part of these correlations is the Auger effect which is a particularly competing process because it does also fill the hole in a low-lying, empty electron state, but which is known to belong to correlations beyond TDLDA [24]. It was shown for N_2 in Ref. [11] that, fortunately, the rate of dissipation is smaller than the growth rate of the instability such that the dipole instability persists, although slightly reduced.

We close with a brief summary. We have investigated the dipole instability that can occur after irradiation by a strong and short XUV pulse. To concentrate on the properties of the instability, we have simplified (as often done) the excitation mechanism by instantaneous generation of a hole in one of the occupied electron states in the molecule. Our findings are:

1. Scanning a variety of molecules and atoms, we find that the dipole instability appears in many and very different systems while it remains absent in many others. We could not yet deduce a simple rule to predict where and where not the instability occurs.
2. The mechanism beyond the dipole instability is very similar to the generation of a coherent photon field in the laser (Mexican hat potential) leading to exponential growth of the dipole envelope with steady oscillations underneath. The oscillations frequency is that of the transition from the hole state to the HOMO.
3. The appearance of the dipole instability depends on the state into which the hole is cut. A hole in the HOMO and states close to it will not produce any instability. Deeper lying states are more likely to do so.
4. Varying the depletion of a hole with dipole instability changes the growth rate and final dipole amplitude (both larger with increasing depletion). But the instability persists to appear, even at low depletion.
5. We have managed to produce a cooled hole state which ends up stable under static iterations constrained to have a hole in the deepest state. The dipole dynamics from the cooled state is almost the same as that from the instantaneous hole. This indicates that the instability is a robust property of the system.

All observations taken together suggest that the appearance of the dipole instability depends on the coupling between the instability mode (oscillations between hole state and HOMO) and other dipole modes in the system. A simple quantitative measure for that has yet to be developed. Research in that direction is underway.

Acknowledgments

For computational resources, we acknowledge support from the RRZE (Regionales Rechenzentrum Erlangen).

References

1. F. Krausz, M. Ivanov, Rev. Mod. Phys. **81**, 163 (2009)
2. F. Calegari, G. Sansone, S. Stagira, C. Vozzi, M. Nisoli, J. Phys. B **49** (2016)
3. M. Kitzler, S. Gräfe, Ultrafast Dynamics Driven by Intense Light Pulses (Springer International Publishing, New York, 2015)
4. D.R. Austin, A.S. Johnson, F. McGrath, D. Wood, L. Miseikis, T. Siegel, P. Hawkins, A. Harvey, Z. Masin, S. Patchkovskii et al., Sci. Rep. **11**, 2485 (2021)
5. R. Weinkauf, P. Schanen, A. Metsala, E.W. Schlag, M. Buergle, H. Kessler, J. Phys. Chem. **100**, 18567 (1996)
6. L. Cederbaum, J. Zobeley, Chem. Phys. Lett. **307**, 205 (1999)
7. F. Remacle, R.D. Levine, E.W. Schlag, R. Weinkauf, J. Phys. Chem. A **103**, 10149 (1999)
8. A.I. Kuleff, N.V. Kryzhevoi, M. Pernpointner, L.S. Cederbaum, Phys. Rev. Lett. **117**, 093002 (2016)
9. C.E.M. Gonçalves, R.D. Levine, F. Remacle, Phys. Chem. Chem. Phys. **23**, 12051 (2021)
10. F. Khalili, M. Vafaee, B. Shokri, Phys. Chem. Chem. Phys. **23**, 23005 (2021)
11. P.G. Reinhard, D. Dundas, P.M. Dinh, M. Vincendon, E. Suraud (2022), arxiv.org/abs/2205.09997
12. L.S. Cederbaum, W. Domcke, J. Schirmer, W.V. Niessen, Adv. Chem. Phys. **65**, 115 (1986)
13. R.M. Dreizler, E.K.U. Gross, Density Functional Theory: An Approach to the Quantum Many-Body Problem (Springer-Verlag, Berlin, 1990)
14. J.P. Perdew, Y. Wang, Phys. Rev. B **45**, 13244 (1992)
15. E. Fermi, E. Amaldi, Accad. Ital. Rome **6**, 117 (1934)
16. C. Legrand, E. Suraud, P.G. Reinhard, J. Phys. B **35**, 1115 (2002)
17. P. Klüpfel, P.M. Dinh, P.G. Reinhard, E. Suraud, Phys. Rev. A **88**, 052501 (2013)
18. P.G. Reinhard, E. Suraud, Theoret. Chem. Acc. **140**, 63 (2021)
19. S. Goedecker, M. Teter, J. Hutter, Phys. Rev. B **54**, 1703 (1996)
20. P.M. Dinh, M. Vincendon, F. Coppens, E. Suraud, P.G. Reinhard, Comput. Phys. Comm. **270**, 108155 (2022)
21. H. Haken, Laser Theory (Springer, Berlin, 1984)

22. P.G. Reinhard, E. Suraud, Ann. Phys. (N.Y.) **354**, 183 (2015)
23. M. Vincendon, E. Suraud, P.G. Reinhard, Eur. Phys. J. D **71**, 179 (2017), https://doi.org/10.1140/epjd/e2017-80067-0
24. C.S. Cucinotta, D. Hughes, P. Ballone, Phys. Rev. B **86**, 045114 (2012)